Nonlinear Dyn (2010) 61: 443–463
DOI 10.1007/s11071-010-9661-2

ORIGINAL PAPER

Relaxation oscillations, subharmonic orbits and chaos in the dynamics of a linear lattice with a local essentially nonlinear attachment

Alexander F. Vakakis

Received: 25 May 2009 / Accepted: 11 January 2010 / Published online: 6 February 2010

Abstract We study the dynamic interactions between traveling waves propagating in a linear lattice and a lightweight, essentially nonlinear and damped local attachment. Correct to leading order, we reduce the dynamics to a strongly nonlinear damped oscillator forced by two harmonic terms. One of the excitation frequencies is characteristic of the traveling wave that impedes to the attachment, whereas the other accounts for local lattice dynamics. These two frequencies are energy-independent; a third energy-dependent frequency is present in the problem, characterizing the nonlinear oscillation of the attachment when forced by the traveling wave. We study this three-frequency strongly nonlinear problem through slow-fast partitions of the dynamics and resort to action-angle coordinates and Melnikov analysis. For damping below a critical threshold, we prove the existence of relaxation oscillations of the attachment; these oscillations are associated with enhanced targeted energy transfer from the traveling wave to the attachment. Moreover, in the limit of weak or no damping, we prove the existence of subharmonic oscillations of arbitrarily large periods, and of chaotic motions. The analytical results are supported by numerical simulations of the reduced order model.

Keywords Essential stiffness nonlinearity · Relaxation oscillations · Subharmonic orbits · Chaotic orbits

1 Introduction

Lattices with local attachments (or "defects") have been studied extensively in the literature, (e.g., [7, 8, 12, 13, 16, 18]), since they appear in extensive applications. These include the areas of granular media and metamaterials [5, 23]; of solid state physics and defect-induced relaxation phenomena in superconductors [4, 15, 17, 21, 27]; and of photonic band-gap materials (photonic crystals) [1, 3, 6].

Considering previous works on lattices with nonlinear attachments, Rothos and Vakakis [25] studied subharmonic motions and chaos in a lattice with a nonlinear attachment in the form of a softening Duffing oscillator with negative linear part. Goodman et al. [13] considered the interaction of nonlinear Schrödinger solitons with a localized defect in a medium of infinite extent, and studied nonlinear resonance energy transfer [28] from the soliton to a localized standing wave at the position of the defect. A fundamental mechanism for energy transfer from dynamical systems to essentially nonlinear attachments is nonlinear resonance capture of the dynamics in invariant manifolds

W. Grafton and Lillian B. Wilkins Professor.

A.F. Vakakis (✉)
Department of Mechanical Science and Engineering,
University of Illinois at Urbana-Champaign,
Urbana-Champaign, IL, USA
e-mail: avakakis@illinois.edu

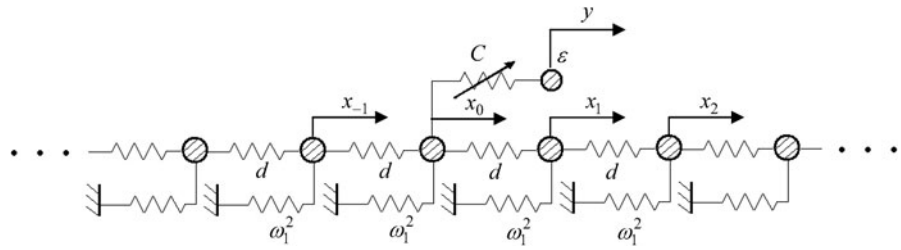

Fig. 1 Linear lattice with strongly nonlinear attachment

of the dynamics [30]. Additional works on soliton-defect nonlinear interactions were performed in [7, 8, 12, 16].

In the present work, we study the strongly nonlinear dynamic interaction between traveling waves propagating in a lattice and a lightweight defect in the form of a nonlinear oscillator with nonlinearizable cubic stiffness nonlinearity of the hardening type. We will employ different techniques ranging from slow-fast partition of the dynamics, complexification, and averaging, to subharmonic and homoclinic Melnikov theory, with the aim to study different regimes of the complex dynamics of this system, such as, relaxation oscillations, countable infinities of subharmonic orbits, and chaotic motions.

2 Derivation of a reduced order model of the dynamics

We consider an infinite linear lattice of mechanical oscillators with a lightweight, essentially nonlinear oscillator attached to the zero-th particle (cf. Fig. 1),

$$\begin{aligned}
&\varepsilon\ddot{y} + \lambda(\dot{y} - \dot{x}_0) + C(y - x_0)^3 = 0\\
&\ddot{x}_0 + \omega_1^2 x_0 + d(2x_0 - x_1 - x_{-1})\\
&\quad = \lambda(\dot{y} - \dot{x}_0) + C(y - x_0)^3\\
&\ddot{x}_n + \omega_1^2 x_n + d(2x_n - x_{n-1} - x_{n+1}) = 0\\
&\quad n = \pm 1, \pm 2, \ldots
\end{aligned} \tag{1}$$

where d and ω_1 denote the coupling and grounding stiffnesses of lattice particles, respectively, and ε the small positive parameter scaling the light mass of the attachment. We note that the attachment possesses *essential* stiffness nonlinearity (of hardening cubic type of coefficient C), and does not possess a linear component. Moreover, the only viscous dissipation in the system is assumed to be in the attachment, with viscous damping coefficient λ (not necessarily small at this point).

First, we consider the dynamics of system (1) in the limit $\varepsilon \to 0$ corresponding to the linear infinite lattice with no attachment. It is well known [20] that the unperturbed, perfectly symmetric lattice supports traveling waves for which the following relation between the lattice coordinates holds:

$$x_n(t) = X_n e^{j\mu} e^{j\omega t} + cc, \quad n = 0, \pm 1, \pm 2, \ldots \tag{2}$$

where $j = (-1)^{1/2}$ and (cc) denotes complex conjugate. The parameter μ in (2) is termed the propagation constant, which for traveling waves is a real quality. Substituting (2) into the equations of motion of the unperturbed infinite lattice (with $\varepsilon = 0$), we compute the propagation constant μ of the traveling wave as function of the frequency ω:

$$\mu = \cos^{-1}\left(1 - \frac{\omega^2 - \omega_1^2}{2d}\right) \tag{3}$$

This relation defines a *propagation zone* (*PZ*) in the frequency domain, namely the frequency range $\omega_1 < \omega < \sqrt{\omega_1^2 + 4d}$ where traveling waves can be realized. At the lower (ω_1) and upper ($\sqrt{\omega_1^2 + 4d}$) bounding frequencies of the PZ, the propagation constant becomes $\mu = +\pi$ and $\mu = -\pi$, respectively, and the traveling waves degenerate to either in-phase or out-of-phase standing waves (which are normal modes of the lattice).

On the contrary, for frequencies in *attenuation zones* (*AZs*), i.e., lying outside the PZ, the propagation constant becomes a purely imaginary quantity and the unperturbed lattice supports only in-phase or out-of-phase standing waves possessing exponentially decaying envelopes. These are near field synchronous motions of the lattice, corresponding to either in-phase relative motions between adjacent lattice particles (in the frequency range $0 < \omega < \omega_1$), or out-of-phase relative motions between particles (in the range $\sqrt{\omega_1^2 + 4d} < \omega$).

We wish to study the dynamic interaction of the lattice dynamics with the essentially nonlinear attachment as ε increases from zero but still remains a small quantity. In particular, we will focus in the dynamical interaction between traveling waves propagating within the PZ of the linear lattice and the lightweight essential nonlinear attachment. Throughout this work and without loss of generality, we will consider initial conditions for system (1) of the form:

$$\begin{aligned} &y(0)=0, \quad \dot{y}(0)=V, \quad x_n(0)=0, \\ &\dot{x}_n(0)=F_n, \quad n=0,\pm1,\pm2,\ldots \end{aligned} \tag{4}$$

Introducing the rescalings,

$$\begin{aligned} &x_n \to \varepsilon^{1/2}x_n, \quad y \to \varepsilon^{1/2}y, \quad F_n \to \varepsilon^{1/2}F_n, \\ &V \to \varepsilon^{1/2}V, \quad n=0,\pm1,\pm2,\ldots \end{aligned} \tag{5}$$

and the new variables, $v = x_0 + \varepsilon y$, $w = x_0 - y$, the two leading equations of system (1) and the corresponding initial conditions in (4) are expressed as follows:

$$\begin{aligned} &\ddot{w} + \left[(1+\varepsilon)\lambda/\varepsilon\right]\dot{w} + C(1+\varepsilon)w^3 = \ddot{v}, \\ &\quad w(0)=0, \dot{w}(0)=F_0-V \\ &\ddot{v} + \left[\left(\omega_1^2+2d\right)/(1+\varepsilon)\right](v+\varepsilon w) = d(x_1+x_{-1}), \\ &\quad v(0)=0, \dot{v}(0)=F_0+\varepsilon V \end{aligned} \tag{6}$$

The variable w denotes the relative response between the nonlinear attachment and the zero-th particle of the lattice (i.e., the particle to which it is attached), whereas, the variable v denotes the motion of the center of mass of the system composed of the attachment and the zero-th particle of the chain.

The pseudo-forcing term in the second of the above equations can be analytically evaluated in terms of the variable w by employing the Green's functions of the linear lattice [31]. This reduces the infinite-dimensional dynamical system (6) into the following form,

$$\begin{aligned} &w'' + \hat{\lambda}w' + \hat{C}(1+\varepsilon)w^3 = v'' \\ &v'' + v + \varepsilon w \\ &\quad = \left(d\Omega^{-2}\right)\sum_{r=-\infty}^{+\infty} F_r\left[G_{1-r}(\tau)+G_{1+r}(\tau)\right] \\ &\qquad - 2\varepsilon d\hat{C}\left[w^3(\tau) * G_1(\tau)\right] \\ &w(0)=0, \quad w'(0)=(F_0-V)\Omega^{-1}, \\ &v(0)=0, \quad v'(0)=(F_0+\varepsilon V)\Omega^{-1} \end{aligned} \tag{7}$$

where the dependent variables are expressed in terms of the normalized time variable $\tau = (\omega_1^2+2d)^{1/2}(1+\varepsilon)^{-1/2}t$; moreover, the normalized coefficients $\Omega^2 = (\omega_1^2+2d)(1+\varepsilon)^{-1}$, $\hat{\lambda} = \lambda(1+\varepsilon)(\varepsilon\Omega)^{-1}$, and $\hat{C} = C\Omega^{-2}$ are introduced, and by $(*)$ we denote the convolution operator. The kernels $G_n(\tau) = G_{-n}(\tau), n \in N$ in (7) are defined by the following expression [31]:

$$\begin{aligned} &G_n(\tau) \\ &\quad = \Omega^{-1}\int_0^\tau J_0\left[\alpha\left(\tau^2-u^2\right)^{1/2}\right]J_{2n}\left(2d^{1/2}u/\Omega\right)du, \\ &\quad n=0,\pm1,\pm2,\ldots \end{aligned} \tag{8}$$

where $\alpha = \omega_1/\Omega$, and $J_p(\bullet)$ is Bessel's function of the first kind and integer order p.

Hence, the dynamics of the infinite-dimensional system (1) can be reduced to the system of integro-differential equations (7). Moreover, the reduced model (7) is exact, as no approximations were made for its derivation. As mentioned previously, traveling waves in the unperturbed lattice propagate with normalized frequencies in the range, $\alpha < \omega/\Omega < [\alpha^2 + 2(1+\varepsilon-\alpha^2)]^{1/2} \equiv \alpha_1$. Based on relations (2), it can be shown that traveling waves in the lattice are realized for initial velocities $F_n = F\cos 2n\theta, 0 < \theta < \pi/2, n = 0,\pm1,\pm2,\ldots$, with the lower limit $\theta = 0$ corresponding to the lower bounding frequency of the PZ (and the in-phase normal mode of the chain, $F_n = F, n = 0,\pm1,\pm2,\ldots$), and the upper limit $\theta = \pi/2$ corresponding to the upper bounding frequency of the PZ (and the out-of-phase normal mode of the lattice, $F_n = (-1)^n F, n = 0,\pm1,\pm2,\ldots$). It follows that angle θ parameterizes the PZ of the lattice, and the frequencies and amplitudes of traveling waves within the PZ. Taking into account relations satisfied by Bessel functions of the first kind [32], we may simplify the infinite summation on the right-hand side of the second of (7) according to

$$\begin{aligned} &\left(d\Omega^{-2}\right)\sum_{r=-\infty}^{+\infty} F_r\left[G_{1-r}(\tau)+G_{1+r}(\tau)\right] \\ &\quad = F\Lambda_\theta \sin\alpha_\theta\tau \end{aligned} \tag{9}$$

with

$$\begin{aligned} &\Lambda_\theta = \frac{2d\cos 2\theta}{\alpha\Omega^3}\left(1+\frac{4d\sin^2\theta}{\alpha^2\Omega^2}\right)^{-1/2}, \\ &\alpha_\theta = \left(1+\frac{4d\sin^2\theta}{\alpha^2\Omega^2}\right)^{1/2}\alpha \end{aligned} \tag{10}$$

Substituting (9) into the second of the equations of the reduced model (7), we express it in the following simplified form:

$$v'' + v = F\Lambda_\theta \sin\alpha_\theta\tau + \varepsilon\left\{-w(\tau) - 2d\hat{C}\left[w^3(\tau) * G_1(\tau)\right]\right\} \quad (11)$$

This is a linear differential equation in v, and taking into account the assumed initial conditions it can be explicitly solved in closed form as follows:

$$v(\tau) = F\left\{\Omega^{-1}\sin\tau + \Lambda_\theta\int_0^\tau \sin\alpha_\theta u \sin(\tau-u)du\right\} + \varepsilon\left\{\left(V\Omega^{-1}\right)\sin\tau + \int_0^\tau\left[-w(u) + 2d\hat{C}\left[w^3(u) * G_1(u)\right]\right]\sin(\tau-u)du\right\} \quad (12)$$

Clearly, the analytical solution above depends on w, so it does not represent a true solution to the problem in terms of v; however, it can help us reduce even further the problem (7). Indeed, substituting (12) into the first of equations (7), *we reduce the dynamics of the traveling wave-nonlinear attachment interaction to a single strongly nonlinear nonhomogeneous equation*:

$$w'' + \hat{\lambda}w' + \hat{C}w^3 = F\left(\frac{\Lambda_\theta\alpha_\theta}{1-\alpha_\theta^2} - \Omega^{-1}\right)\sin\tau - \frac{F\Lambda_\theta\alpha_\theta^2}{1-\alpha_\theta^2}\sin\alpha_\theta\tau + O(\varepsilon)$$
$$0 < \theta < \pi/2,\ w(0) = 0,\ w'(0) = (F-V)\Omega^{-1} \quad (13)$$

We note that the reduced model (13) is approximate since terms of $O(\varepsilon)$ are omitted; these higher order terms contain convolutions in terms of w rendering the reduced model an integro-differential equation. However, to leading order the model (13) is in the form of an ordinary differential equation (albeit strongly nonlinear), which simplifies considerably the analysis.

In conclusion, to leading order the relative motion of the lightweight attachment with respect to the zeroth particle of the lattice is governed by a strongly nonlinear oscillator forced by two harmonic terms representing to excitation of the nonlinear attachment by impeding traveling waves. The first harmonic of the excitation is at normalized frequency equal to unity and characterizes the local lattice dynamics (i.e., the grounded stiffness of each particle of the lattice), whereas the second harmonic corresponds to the normalized frequency of the traveling wave inside the normalized PZ, $\alpha < \alpha_\theta < [\alpha^2 + 2(1-\alpha^2)]^{1/2} + O(\varepsilon)$. Hence, the model (13) accounts only for the excitation of the nonlinear attachment by the traveling wave in the lattice, and not for the 'reaction dynamics' of the nonlinear attachment which is modeled by the higher order terms in the form of convolution operators in w. By the previous asymptotic formulation, however, these higher order effects are small as $\varepsilon \to 0$. We note that as the frequency of the traveling wave approaches the bounding frequencies of the propagation zone of the chain, the problem changes and degenerates to the problem of resonance interaction of standing waves (normal modes) of the chain with the nonlinear attachment. Then higher order terms should be included in the asymptotic analysis in order to accurately characterize that resonance interaction. This problem, however, is not considered in this work.

Our further study, and unless otherwise noted, will focus on the strongly nonlinear reduced model (13) under the assumption of weak inter-particle coupling. To this end, we rescale the coupling parameter of the lattice according to $d = \varepsilon^{1/4}D$ and express the normalized frequency of the second harmonic of the excitation term as

$$\alpha_\theta = 1 - \varepsilon^{1/4}D\omega_1^{-2}\cos 2\theta + O\left(\varepsilon^{1/2}\right) \equiv 1 + \varepsilon^{1/4}B(\theta) + O\left(\varepsilon^{1/2}\right) \quad (14)$$

where $B(\theta) = -D\omega_1^{-2}\cos 2\theta$ is a normalized frequency detuning parameter. For simplicity, we will focus in the case where the amplitudes of the two harmonic terms in the nonhomogeneous term of (13) are equal, i.e., we will be concerned only with the specific angles $\theta = \bar{\theta}$ satisfying the relation,

$$\left.\frac{\Lambda_\theta\alpha_\theta}{1-\alpha_\theta^2} - \Omega^{-1}\right|_{\theta=\bar{\theta}} = \left.-\frac{\Lambda_\theta\alpha_\theta^2}{1-\alpha_\theta^2}\right|_{\theta=\bar{\theta}} \quad (15)$$

and corresponding to frequency detuning $B(\bar{\theta}) \equiv \bar{B}$. In Fig. 2, we depict the dependence of $\bar{\theta}$ on the small parameter ε in the limit of weak interparticle coupling $d = \varepsilon^{1/4}D$ for $D = \omega_1 = 1.0$; we note that for small ε it holds that $\bar{B} < 0$. By imposing relation (15), the nonlinear attachment is excited by two harmonic terms of equal magnitude and closely spaced normalized frequencies equal to 1 and $(1 + \varepsilon^{1/4}\bar{B})$; as dis-

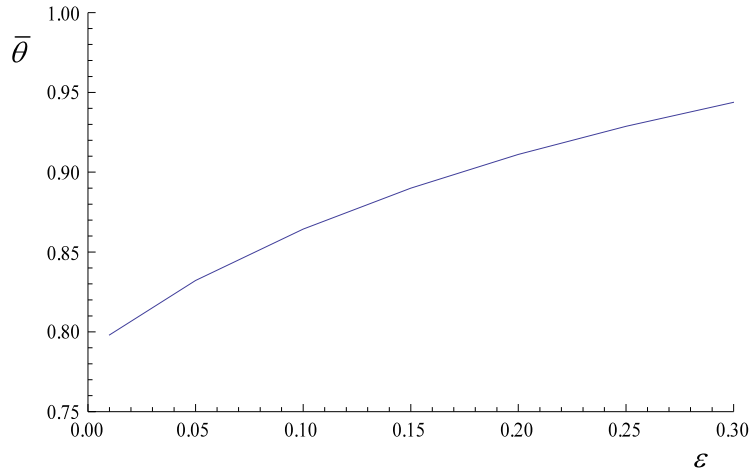

Fig. 2 Angle $\bar{\theta}$ as function of the small parameter ε for $D = 1.0$ and $\omega_1 = 1.0$

cussed below this paves the wave for slow-fast partitioning of the dynamics as these are expected to be in the form of "slowly" modulated "fast" oscillations. As mentioned previously, the first frequency characterizes the grounding stiffness of each particle of the lattice, whereas the second is characteristic of the traveling wave impeding to the nonlinear attachment.

Taking these assumptions into consideration, in the limit of weak interparticle coupling the reduced model (13) is expressed as

$$\begin{aligned} &w'' + \hat{\lambda} w' + \hat{C} w^3 \\ &\quad = \hat{F} \sin\tau + \hat{F} \sin\left(1 + \varepsilon^{1/4} \bar{B}\right)\tau + O(\varepsilon) \\ &\quad = \hat{F}\left[1 + \cos\left(\varepsilon^{1/4} \bar{B}\tau\right)\right] \sin\tau \\ &\qquad + \hat{F} \sin\left(\varepsilon^{1/4} \bar{B}\tau\right) \cos\tau + O(\varepsilon) \\ &\quad w(0) = 0,\ w'(0) = F - V \end{aligned} \tag{16a}$$

where from now on we set $\omega_1 = 1$, and define the common amplitude of the two harmonics as

$$\hat{F} = \left.\frac{-F \Lambda_\theta \alpha_\theta^2}{1 - \alpha_\theta^2}\right|_{\theta = \bar{\theta}} \tag{16b}$$

We note that in the limit of weak interparticle coupling of the lattice the forcing terms are partitioned in terms of "slow" components with normalized frequency $\varepsilon^{1/4} \bar{B}$, and "fast" components with normalized frequency equal to unity. It follows that the problem renders itself to the complexification-averaging (CX-A) analysis first developed by Manevitch [19] (see also [29] for an extensive series of further applications), based on slow-fast partition of the nonlinear dynamics. As shown in these works, the CX-A methodology is suitable for the analysis of strongly nonlinear transient or steady state problems of the type discussed herein. In the following sections, we will analyze the dynamical system (16), and show that depending on its damping it exhibits different response regimes and complex dynamical behavior, such as relaxation oscillations, countable infinities of subharmonic orbits, and chaotic motions.

3 Relaxation oscillations

We now apply the CX-A method developed by Manevitch [19] to the analysis of the reduced order model (16a). We start by introducing the new complex variable,

$$\psi(\tau) = w'(\tau) + j w(\tau) \tag{17}$$

where $j = (-1)^{1/2}$. The reduced model is then expressed in the following complex form:

$$\begin{aligned} &\psi' - \frac{j}{2}\left(\psi + \psi^*\right) + \frac{\hat{\lambda}}{2}\left(\psi + \psi^*\right) + \frac{j\hat{C}}{8}\left(\psi - \psi^*\right)^3 \\ &\quad = \hat{F}\left[\frac{e^{j\tau} - e^{-j\tau}}{2j}\right] \\ &\qquad + \hat{F}\left[\frac{e^{j(1+\varepsilon^{1/4}\bar{B})\tau} - e^{-j(1+\varepsilon^{1/4}\bar{B})\tau}}{2j}\right] + O(\varepsilon) \end{aligned} \tag{18}$$

We represent the solution of (18) in the form,

$$\psi(\tau) = \varphi(\tau) e^{j\tau} \tag{19}$$

where $\varphi(\tau)$ is a slowly varying complex amplitude that modulates the fast oscillation $e^{j\tau}$. This *ansatz* is dictated by the slow-fast partition of the nonhomogeneous term of (16a), and by the recognition that there exists a single fast frequency in the dynamics (whose normalized value is unity). Substituting (19) into (18) and averaging out fast frequency components with frequencies higher than unity we obtain the following complex modulation equation governing the slow evolution of $\varphi(\tau)$:

$$\begin{aligned} &\varphi' + \frac{j}{2}\varphi + \frac{\hat{\lambda}}{2}\varphi - \frac{3j\hat{C}}{8}|\varphi|^2\varphi \approx \frac{\hat{F}}{2j}\left(1 + e^{j\varepsilon^{1/4}\bar{B}\tau}\right) \\ &\varphi(0) = F - V \end{aligned} \tag{20}$$

To proceed with our analysis, we introduce the polar transformation $\varphi(\tau) = N(\tau)e^{j\eta(\tau)}$, substitute into (20) and set separately equal to zero the real and imaginary parts of the resulting expression:

$$\begin{aligned} N' &= \left(\hat{F}/2\right)\sin\left(\varepsilon^{1/4}\bar{B}\tau - \eta\right) - \left(\hat{\lambda}/2\right)N - \left(\hat{F}/2\right)\sin\eta \\ N\eta' &= \left(-\hat{F}/2\right)\cos\left(\varepsilon^{1/4}\bar{B}\tau - \eta\right) \\ &\quad - (N/2) + \left(3\hat{C}/8\right)N^3 - \left(\hat{F}/2\right)\cos\eta \end{aligned} \tag{21}$$

This is a set of real nonlinear differential equations that we proceed to analyze using the method of multiple scales [22]. To this end, we introduce the fast time scale $\tau_0 = \tau$ and the slow time scales $\tau_1 = \varepsilon^{1/4}\tau$, $\tau_2 = \varepsilon^{2/4}\tau, \ldots$, and express the amplitude and phase in (21) in the following series:

$$\begin{aligned} N(\tau) &= N(\tau_0, \tau_1, \ldots) \\ &= N_0(\tau_0, \tau_1, \ldots) + \varepsilon^{1/4}N_1(\tau_0, \tau_1, \ldots) + \cdots \\ \eta(\tau) &= \eta(\tau_0, \tau_1, \ldots) \\ &= \eta_0(\tau_0, \tau_1, \ldots) + \varepsilon^{1/4}\eta_1(\tau_0, \tau_1, \ldots) + \cdots \end{aligned} \tag{22}$$

In the method of multiple scales, the new time scales are treated as *independent variables*. Substituting (22) into (21), expressing the derivatives in terms of the new time scales and matching terms at different orders of magnitude, we obtain an hierarchy of problems governing the successive approximations in (22).

The $O(1)$ subproblem is governed by the following system:

$$\begin{aligned} \frac{\partial N_0}{\partial \tau_0} &= \frac{\hat{F}}{2}\sin\left(\bar{B}\tau_1 - \eta_0\right) - \frac{\hat{\lambda}N_0}{2} - \frac{\hat{F}}{2}\sin\eta_0 \\ \frac{\partial \eta_0}{\partial \tau_0} &= -\frac{\hat{F}}{2}\cos\left(\bar{B}\tau_1 - \eta_0\right) - \frac{N_0}{2} \\ &\quad + \frac{3\hat{C}N_0^3}{8} - \frac{\hat{F}}{2}\cos\eta_0 \end{aligned} \tag{23}$$

We wish to study the *steady state dynamics of this system in terms of the fast time scale* τ_0. This is performed by examining the limit of the dynamics of (23) as $\tau_0 \to \infty$ and setting partial derivatives with respect to τ_0 equal to zero. Clearly, the steady state dynamics in terms of the fast time scale may still be unsteady with respect to the slow time scale τ_1 and higher order time scales, but this is acceptable since the different time scales are treated as independent variables. It follows that as $\tau_0 \to \infty$ the dynamics is governed by the system of equations,

$$\begin{aligned} &\frac{\hat{F}}{2}\sin\left(\bar{B}\tau_1 - \hat{\eta}_0\right) - \frac{\hat{\lambda}\hat{N}_0}{2} - \frac{\hat{F}}{2}\sin\hat{\eta}_0 = 0 \\ &-\frac{\hat{F}}{2}\cos\left(\bar{B}\tau_1 - \hat{\eta}_0\right) - \frac{\hat{N}_0}{2} + \frac{3\hat{C}\hat{N}_0^3}{8} - \frac{\hat{F}}{2}\cos\hat{\eta}_0 = 0 \\ &(\tau_0 \to \infty) \end{aligned} \tag{24}$$

where the steady state amplitude and phase (in terms of the fast time scale) are slowly varying quantities, defined as $\hat{N}_0(\tau_1, \ldots) = \lim_{\tau_0 \to \infty} N_0(\tau_0, \tau_1, \ldots)$ and $\hat{\eta}_0(\tau_1, \ldots) = \lim_{\tau_0 \to \infty} \eta_0(\tau_0, \tau_1, \ldots)$. Manipulating expressions (24), we express $\hat{\eta}_0$ as a function of $\hat{N}_0$,

$$\begin{aligned} \sin\hat{\eta}_0 = \Bigg\{ &-\frac{\hat{\lambda}\hat{N}_0}{\hat{F}}\left(1 + \cos\bar{B}\tau_1\right) \\ &+ \left(-\frac{\hat{N}_0}{\hat{F}} + \frac{3\hat{C}\hat{N}_0^3}{4\hat{F}}\right)\sin\bar{B}\tau_1 \Bigg\} \\ &\times \left[\left(1 + \cos\bar{B}\tau_1\right)^2 + \sin^2\bar{B}\tau_1\right]^{-1} \end{aligned} \tag{25}$$

with $\hat{N}_0$ governed by the algebraic relation:

$$\left(\frac{\hat{N}_0}{\hat{F}}\right)^2\left[\hat{\lambda}^2 + \left(1 - \frac{3\hat{C}\hat{N}_0^2}{4}\right)^2\right]$$

$$
\begin{aligned}
&-2\big(1+\cos\bar{B}\tau_1\big)=0 \quad \Rightarrow \\
&\hat{N}_0^6-\frac{24}{9\hat{C}}\hat{N}_0^4+\frac{16(1+\hat{\lambda}^2)}{9\hat{C}^2}\hat{N}_0^2 \\
&-\frac{32\hat{F}^2}{9\hat{C}^2}\big(1+\cos\bar{B}\tau_1\big)=0
\end{aligned}
\tag{26}
$$

In the terminology of Gendelman and collaborators [9–11], but also see [29]—this represents a *slow invariant manifold—SIM* of the dynamics of system (16a) or (20), i.e., this is the manifold reached asymptotically by the dynamics as $\tau_0 \to \infty$. As indicated by the explicit dependence of relation (26) on the slow time scale τ_1 (but also by the implicit dependence $\hat{N}_0 = \hat{N}_0(\tau_1)$), the SIM is unsteady with respect to the slow time scales, so it provides only a leading order approximation to the exact steady state dynamics of the system. What allows us to express the SIM in the form (26) is the fact that different time scales are treated as independent variables in the multiple scales analysis.

Relation (26) is a cubic polynomial in terms of $\hat{N}_0^2$, so depending on the parameters of the problem it can possess as many as three real solutions for the slowly varying amplitude. Indeed, the (slowly varying) bifurcation surface in parameter space that separates the regimes of one and three real solutions for $\hat{N}_0^2$ can be explicitly computed as

$$
\begin{aligned}
&\left[\frac{16(1+\hat{\lambda}^2)}{27\hat{C}^2}-\frac{576}{729\hat{C}^2}\right]^3+\left[-\frac{64(1+\hat{\lambda}^2)}{243\hat{C}^3}\right. \\
&\left.+\frac{16\hat{F}^2(1+\cos\bar{B}\tau_1)}{9\hat{C}^2}+\frac{1}{27}\left(\frac{24}{9\hat{C}}\right)^3\right]^2=0 \quad \Rightarrow
\end{aligned}
$$

$$
D\big(\hat{\lambda}^2,\hat{C},\hat{F},\bar{B}\tau_1\big)=0 \tag{27}
$$

We note that for fixed nonlinear coefficient $\hat{C}$, forcing amplitude $\hat{F}$ and detuning parameter $\bar{B}$, the leading order dynamics possesses a single solution for $\hat{N}_0^2$ for sufficiently strong damping, and three solutions for damping below a critical slowly varying threshold. The existence of multiple solutions for relatively weak damping has important implications on the dynamics as discussed later. Once the amplitude of the oscillation on the SIM $\hat{N}_0 = \hat{N}_0(\tau_1)$ is computed, the first order approximation to the phase is computed through relation (25).

Corrections to the dynamics on the SIM are computed by considering higher order subproblems. At $O(\varepsilon^{1/4})$ the dynamics is governed by the following system:

$$
\begin{aligned}
\frac{\partial N_1}{\partial\tau_0}&=-\frac{\partial N_0}{\partial\tau_1}-\frac{\eta_1\hat{F}}{2}\cos\big(\bar{B}\tau_1-\eta_0\big)-\frac{\hat{\lambda}N_1}{2} \\
&\quad-\frac{\eta_1\hat{F}}{2}\cos\eta_0 \\
\frac{\partial\eta_1}{\partial\tau_0}&=-\frac{\partial\eta_0}{\partial\tau_1}-\frac{\eta_1\hat{F}}{2}\sin\big(\bar{B}\tau_1-\eta_0\big)-\frac{N_1}{2} \\
&\quad+\frac{9\hat{C}N_0^2N_1}{8}+\frac{\eta_1\hat{F}}{2}\sin\eta_0
\end{aligned}
\tag{28}
$$

To restrict the dynamics on the SIM (i.e., in the limit $\tau_0 \to \infty$), we set the partial derivatives with respect to the fast time τ_0 equal to zero and solve the resulting set of equations in terms of the limits $\hat{N}_1(\tau_1) = \lim_{\tau_0\to\infty} N_1(\tau_0,\tau_1,\ldots)$ and $\hat{\eta}_1(\tau_1) = \lim_{\tau_0\to\infty}\eta_1(\tau_0,\tau_1,\ldots)$:

$$
\begin{Bmatrix}\hat{N}_1\\ \hat{\eta}_1\end{Bmatrix}=\begin{bmatrix}\hat{\lambda}/2 & \big(\hat{F}/2\big)\big[\cos\big(\bar{B}\tau_1-\hat{\eta}_0\big)+\cos\hat{\eta}_0\big]\\ (1/2)\big[1-\big(9\hat{C}\hat{N}_0^2/4\big)\big] & \big(\hat{F}/2\big)\big[\sin\big(\bar{B}\tau_1-\hat{\eta}_0\big)-\sin\hat{\eta}_0\big]\end{bmatrix}^{-1}\begin{Bmatrix}-\frac{\partial\hat{N}_0}{\partial\tau_1}\\ -\frac{\partial\hat{\eta}_0}{\partial\tau_1}\end{Bmatrix} \tag{29}
$$

The approximate steady state dynamics of system (16a) on the SIM is then computed as follows:

$$
\begin{aligned}
w(\tau)&\sim\hat{w}\big(\varepsilon^{1/4}\tau\big)\\
&=\big[\hat{N}_0\big(\varepsilon^{1/4}\tau\big)+\varepsilon^{1/4}\hat{N}_1\big(\varepsilon^{1/4}\tau\big)+O\big(\varepsilon^{1/2}\big)\big]\\
&\quad\times\sin\big[\tau+\hat{\eta}_0\big(\varepsilon^{1/4}\tau\big)+\varepsilon^{1/4}\hat{\eta}_1\big(\varepsilon^{1/4}\tau\big)\\
&\quad+O\big(\varepsilon^{1/2}\big)\big],\quad \tau\gg1
\end{aligned}
\tag{30}
$$

We note that since the above analysis concerns only the dynamics on the SIM and is carried out in the limit of large values of the fast time scale; it does

not necessarily satisfy the initial condition of the problem (16a). The initial value problem is analyzed later.

In Fig. 3, we depict the envelope $|\varphi(\tau)|$ of the steady state oscillation derived by direct numerical simulation of system (20) with parameters $\hat{C}=1$, $\hat{F}=0.3$, $\bar{B}=1$, $\varepsilon=0.05$, and varying values of the damping coefficient $\hat{\lambda}$. For comparison purposes, we superimpose to these plots the theoretical approximations derived by solving (26). For relatively strong damping (cf. Fig. 3a), the envelope is a low-amplitude periodic oscillation, and the corresponding motion $w(\tau)$ of the dynamical system (16a) possesses two closely spaced frequencies; depending on the value of $\varepsilon^{1/4}\bar{B}$ the steady state oscillation of (16a) is either periodic (when $\varepsilon^{1/4}\bar{B}$ is rational—as is the case for the case considered in Fig. 3a) or quasiperiodic (when $\varepsilon^{1/4}\bar{B}$ is irrational). By decreasing the value of damping, the system enters into a regime of *relaxation oscillations* as evidenced by the simulations depicted in Figs. 3b, c. The relaxation oscillations are generated by the multivalued feature of the SIM, which now includes an unstable branch. This gives rise to jumps in the envelope of the steady state dynamics, as the slow motion of the envelope is interrupted by fast transitions between disjoint branches of the SIM. Moreover, the regime of relaxation oscillations is associated with relatively large amplitudes of the attachment. As shown in [26], the energy absorbed and locally dissipated by the nonlinear attachment is approximately proportional to the time integral of the envelope $|\varphi(\tau)|$, so relaxation oscillations are associated with enhanced targeted energy transfer from the impeding traveling waves of the lattice to the strongly nonlinear attachment. A general trend of the results depicted in Fig. 3 is that with diminishing damping the steady state dynamics diverge from the $O(1)$ theoretical prediction; this is evidenced by the increasingly higher-amplitude and higher-frequency oscillations that are superimposed to the SIM oscillation as $\hat{\lambda}\to 0$. This indicates that with diminishing damping the SIM approximation becomes increasingly less valid and higher order effects must be taken into account.

This conclusion is supported by the simulation depicted in Fig. 4 where the envelope of the steady state dynamics is depicted in the limit of no damping ($\hat{\lambda}=0$). We deduce that in the limit of no damping the temporal evolution of the envelope is complex (in fact it seems to be chaotic), and the theoretical SIM prediction is not valid any more. This result provides us with ample motivation for studying the dynamics of system (16) in the limit of weak or no damping.

4 Chaotic motions

Reconsidering the modulation equation (20), we rescale the damping coefficient according to $\hat{\lambda}\to\varepsilon^{1/4}\hat{\lambda}$ in order to consider the case of weak damping,

$$\begin{aligned}&\varphi'+\frac{j}{2}\varphi+\frac{\varepsilon^{1/4}\hat{\lambda}}{2}\varphi-\frac{3j\hat{C}}{8}|\varphi|^2\varphi\approx\frac{\hat{F}}{2j}\left(1+e^{j\gamma}\right)\\&\gamma'=\varepsilon^{1/4}\bar{B}\end{aligned}\tag{31}$$

subject to initial conditions $\varphi(0)=F-V\equiv W$, $\gamma(0)=\bar{\gamma}\in[0,2\pi)$. In this case, however, instead of decomposing the dynamics in terms of slow and fast components and studying the slow dynamics on the SIM (as was performed in the previous section), we focus in the unstable branch of the SIM and study the breakdown of the homoclinic manifolds associated with this branch for slow variation of the angle γ, which leads to chaotic dynamics. We will study the dynamics of (31) in parameter ranges for which the unstable branch of the SIM exists for all values of the phase parameter γ; this is required for the homoclinic Melnikov analysis that will be developed below. Considering the dynamical system (31), in the limit $\varepsilon\to 0$ we obtain an *integrable* dynamical system with no damping and $\gamma=\bar{\gamma}$ fixed. Introducing the transformation $\varphi(\tau)=N(\tau)e^{j\eta(\tau)}$ into (31) and decomposing in terms of real and imaginary parts we obtain the following relations satisfied by the equilibrium points (N_e,η_e) of the integrable system,

$$\begin{aligned}0&=\left(\hat{F}/2\right)\sin(\bar{\gamma}-\eta_e)-\left(\hat{F}/2\right)\sin\eta_e\\0&=\left(\hat{F}/2\right)\cos(\bar{\gamma}-\eta_e)-(N_e/2)\\&\quad+\left(3\hat{C}/8\right)N_e^3-\left(\hat{F}/2\right)\cos\eta_e\end{aligned}\tag{32a}$$

or by eliminating the stationary phase ,

$$(N_e/2)-\left(3\hat{C}/8\right)N_e^3=-\left(\hat{F}/\sqrt{2}\right)\sqrt{1+\cos^2\bar{\gamma}}\tag{32b}$$

It follows that the existence of an unstable equilibrium in the integrable dynamics for all values of $\bar{\gamma}$ corre-

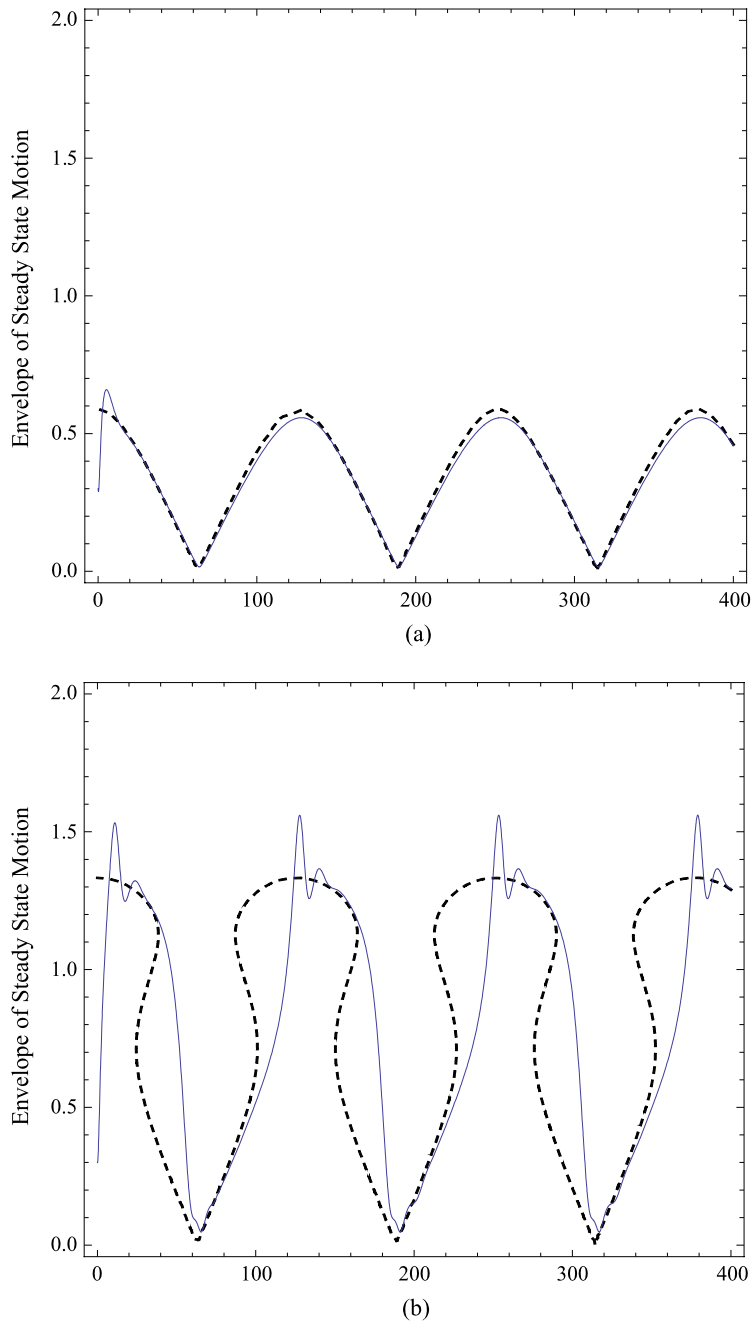

Fig. 3 Envelopes of steady motions for $\hat{C} = 1.0$, $\hat{F} = 0.3$, $\bar{B} = 1.0$, $\varepsilon = 0.05$ and, (**a**) $\hat{\lambda} = 0.7$, (**b**) $\hat{\lambda} = 0.3$, (**c**) $\hat{\lambda} = 0.1$; (*solid line*) $|\varphi(\tau)|$ (numerical simulation), (*dashed line*) $\hat{N}_0(\varepsilon^{1/4}\tau)$ (SIM approximation)

sponds to regions of system parameters where three roots for N_e exist. This holds when $\hat{F} < 2/(9\sqrt{\hat{C}})$, i.e., for sufficiently small forcing amplitudes. In the numerical applications later in this Section we will set $\hat{C} = 4/3$, which leads to the requirement $\hat{F} < 0.192$. Hence, the following analysis is valid for sufficiently small forcing amplitudes below this limit.

Considering again the *integrable* dynamical system (31) with $\varepsilon \to 0$ and no damping, setting $\gamma = \bar{\gamma}$ fixed and assuming that $\hat{F}$ is sufficiently small for the unstable branch of the SIM to exist for all values of $\bar{\gamma}$, we explicitly compute the homoclinic manifold of the unstable branch of the SIM. Indeed, following the analysis in [26], it can be shown that the unperturbed system

Fig. 3 (*Continued*)

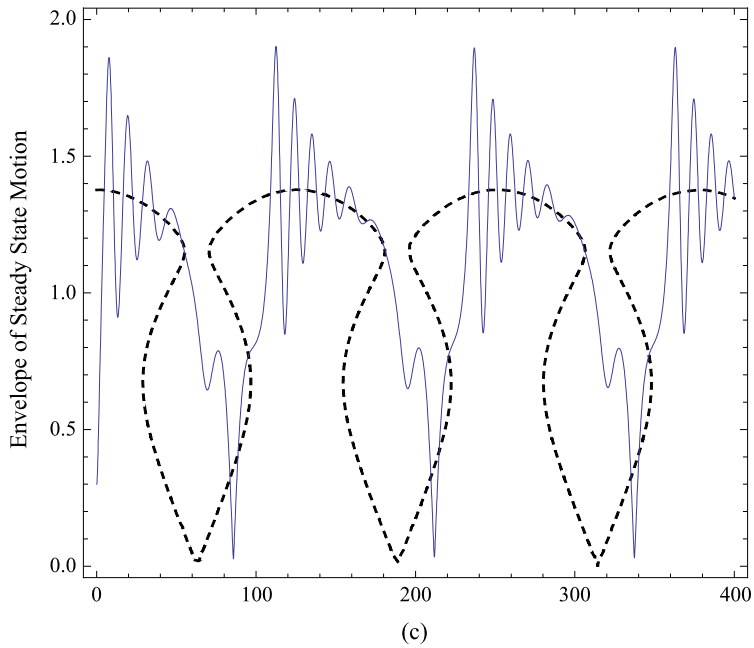

Fig. 4 Envelope of steady state motion for $\hat{C} = 1.0$, $\hat{F} = 0.3$, $\bar{B} = 1.0$, $\varepsilon = 0.05$, and $\hat{\lambda} = 0$; (*solid line*) $|\varphi(\tau)|$ (numerical simulation), (*dashed line*) $\hat{N}_0(\varepsilon^{1/4}\tau)$ (SIM approximation)

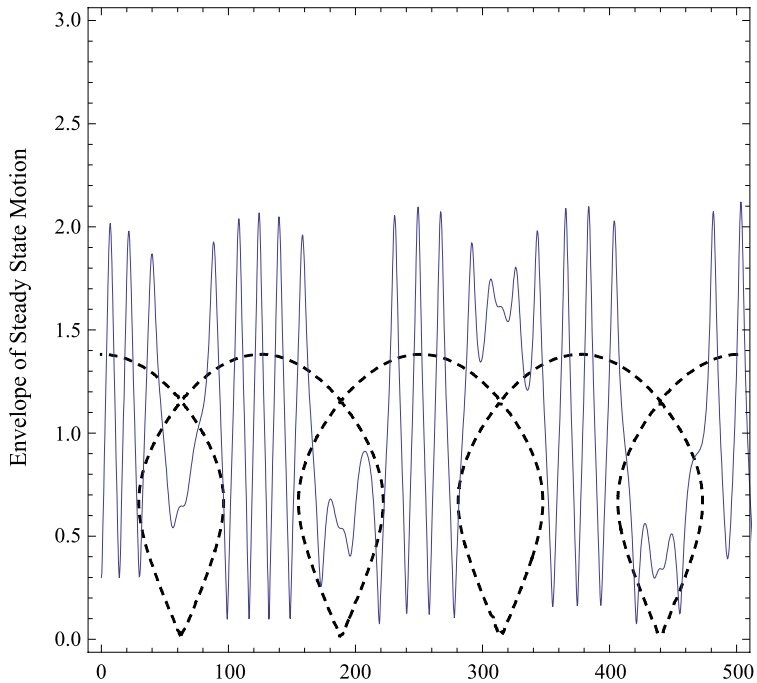

possesses the following first integral of motion,

$$\frac{j}{2}|\varphi|^2 - \frac{3j\hat{C}}{16}|\varphi|^4 - \frac{\hat{F}}{2}\left[\sin\bar{\gamma} - j(1+\cos\bar{\gamma})\right]\varphi^* + \frac{\hat{F}}{2}\left[\sin\bar{\gamma} + j(1+\cos\bar{\gamma})\right]\varphi = 2jH(\bar{\gamma}) \tag{33a}$$

where the right-hand side is a $\bar{\gamma}$-dependent constant of integration. Using the first integral (33a), we may

compute the exact solution of the unperturbed dynamical system.

This is performed by introducing again the polar representation $\varphi(\tau) = N(\tau)e^{j\eta(\tau)}$ leading to the real first order system,

$$N' = \frac{\hat{F}}{2}\big[\sin\bar{\gamma}\cos\eta - (1+\cos\bar{\gamma})\sin\eta\big] \tag{33b}$$

which is complemented by the first integral,

$$\frac{N^2}{2} - \frac{3\hat{C}N^4}{16} + \hat{F}N\big[\sin\bar{\gamma}\sin\eta + (1+\cos\bar{\gamma})\cos\eta\big] = \frac{W^2}{2} - \frac{3\hat{C}W^4}{16} + \hat{F}W(1+\cos\bar{\gamma}) \tag{33c}$$

In (33b, c), we impose the initial conditions $N(0) = W$ and $\eta(0) = 0$. Manipulating these two equations, we may eliminate the angle η and derive an integrable first order equation for the amplitude $N(\tau)$. Setting $N^2(\tau) = z(\tau)$ this equation is expressed as

$$\begin{aligned} z' = &\left\{4\hat{F}^2 z\left[1 + \frac{\sin^2\bar{\gamma}}{(1+\cos\bar{\gamma})^2}\right]^{-1}\right. \\ &- \left[\frac{W^2 - z}{2} - \frac{3\hat{C}}{16}\big(W^4 - z^2\big)\right. \\ &\left.\left. + \hat{F}W(1+\cos\bar{\gamma})\right]^2\right\}^{1/2} \\ \equiv &\big\{Q\big(z, W, \hat{F}, \bar{\gamma}\big)\big\}^{1/2} \end{aligned} \tag{34}$$

with initial condition $z(0) = W^2$. We note that $Q(z, W, \hat{F}, \bar{\gamma})$ is periodic in $\bar{\gamma}$ with period 2π, and satisfies $Q(z, W, \hat{F}, \pi - \nu) = Q(z, W, \hat{F}, \pi + \nu)$, i.e., is symmetric with respect to the line $\bar{\gamma} = \pi$. Moreover, (34) is exactly solved by quadratures,

$$z' = \big\{Q\big(z, W, \hat{F}, \bar{\gamma}\big)\big\}^{1/2} \quad \Rightarrow \quad \int^{z} \frac{dz}{\{Q(z, W, \hat{F}, \bar{\gamma})\}^{1/2}} = \int^{\tau} d\tau + L \tag{35}$$

where L is an integration constant. Clearly, the type of solutions of (35) depends on the roots of the denominator $Q(z, W, \hat{F}, \bar{\gamma})$ which is a quartic polynomial in terms of z. Depending on the system parameters $Q(z, W, \hat{F}, \bar{\gamma})$ generically possesses two or four real roots in z, corresponding to time-periodic solutions for $z(\tau)$. In this section, however, we will consider $\hat{F}$ and $\bar{\gamma}$ to be fixed, and we focus in the degenerate case corresponding to the critical value of the initial condition $W = W_{cr}(\bar{\gamma})$ for which $Q(z, W = W_{cr}(\bar{\gamma}), \hat{F}, \bar{\gamma})$ possesses a pair of coincident real roots and two additional distinct real roots for z. We will assume that these real roots are ordered according to $z_0(\bar{\gamma}) < z_1(\bar{\gamma}) < z_2(\bar{\gamma})$, where $z_1(\bar{\gamma})$ is the double root.

Then it can be shown that the dynamical system (34) possesses a degenerate pair of homoclinic orbits which can be explicitly computed [14]. Indeed, following an analysis similar to [26], one of the homoclinic orbits is computed as

$$z^{(h)}(\tau;\bar{\gamma}) = N^{(h)^2}(\tau;\bar{\gamma}) = z_1(\bar{\gamma}) - \frac{g_1(\bar{\gamma})g_2(\bar{\gamma})}{g_1(\bar{\gamma})\sinh^2[\frac{3\hat{C}\sqrt{g_1(\bar{\gamma})g_2(\bar{\gamma})}}{32}(\tau \pm M(\bar{\gamma}))] + g_2(\bar{\gamma})\cosh^2[\frac{3\hat{C}\sqrt{g_1(\bar{\gamma})g_2(\bar{\gamma})}}{32}(\tau \pm M(\bar{\gamma}))]} \tag{36a}$$

for $\tau \geq 0$, with $g_1(\bar{\gamma}) = z_1(\bar{\gamma}) - z_0(\bar{\gamma}), g_2(\bar{\gamma}) = z_2(\bar{\gamma}) - z_1(\bar{\gamma})$. The quantity $M(\bar{\gamma}))$ in the denominator is defined by

$$M(\bar{\gamma}) = -\frac{16}{3\hat{C}}\int_{W_{cr}^2(\bar{\gamma})}^{z_0(\bar{\gamma}))} \frac{du}{[z_1(\bar{\gamma}) - u]\{[u - z_0(\bar{\gamma})][z_2(\bar{\gamma}) - u]\}^{1/2}} > 0 \tag{36b}$$

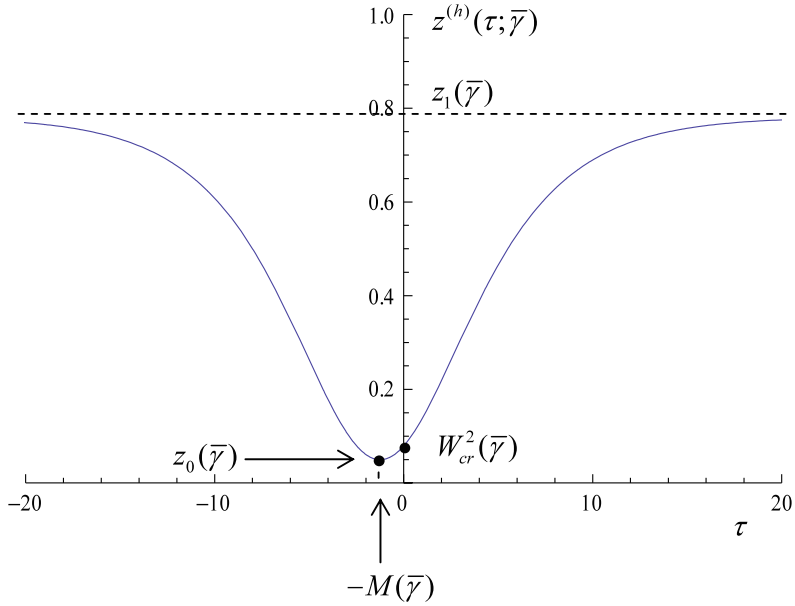

(a)

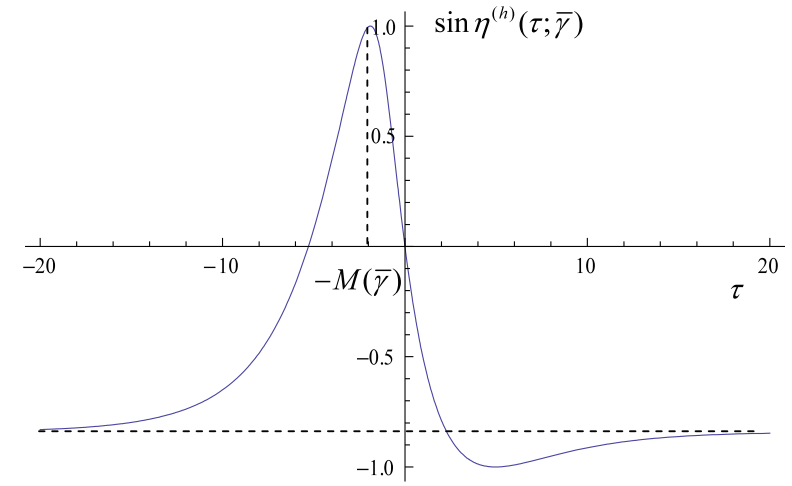

(b)

Fig. 5 Homoclinic orbit of the unperturbed system (31) ($\varepsilon = 0$) for $\hat{F} = 0.1786$, $\hat{C} = 4/3$, $\bar{\gamma} = 2.0$, $W_{cr}(\bar{\gamma}) = 0.281519$: (**a**) $z^{(h)}(\tau;\bar{\gamma})$, (**b**) $\eta^{(h)}(\tau;\bar{\gamma})$, (**c**) representation in the complex plane

with $z_0(\bar{\gamma}) \le W_{cr}^2(\bar{\gamma}) \le z_1(\bar{\gamma}) < z_2(\bar{\gamma})$) and the (+) or (−) sign corresponding to positive or negative values of $W_{cr}(\bar{\gamma})$. The corresponding expression for the phase on the homoclinic solution is given by

$$\sin\eta^{(h)}(\tau;\bar{\gamma}) = \hat{F}^{-1}\frac{d\sqrt{z^h(\tau,\bar{\gamma})}}{d\tau} + \frac{\sin\bar{\gamma}}{2\hat{F}(1+\cos\bar{\gamma})\sqrt{z^h(\tau,\bar{\gamma})}} \times \left\{ \frac{W_{cr}^2(\bar{\gamma}) - z^h(\tau,\bar{\gamma})}{2} - \frac{3\hat{C}}{16}\left[W_{cr}^2(\bar{\gamma}) - z^{h\,2}(\tau,\bar{\gamma})\right] + \hat{F}W_{cr}(\bar{\gamma})(1+\cos\bar{\gamma}) \right\} \quad (37)$$

Fig. 5 (*Continued*)

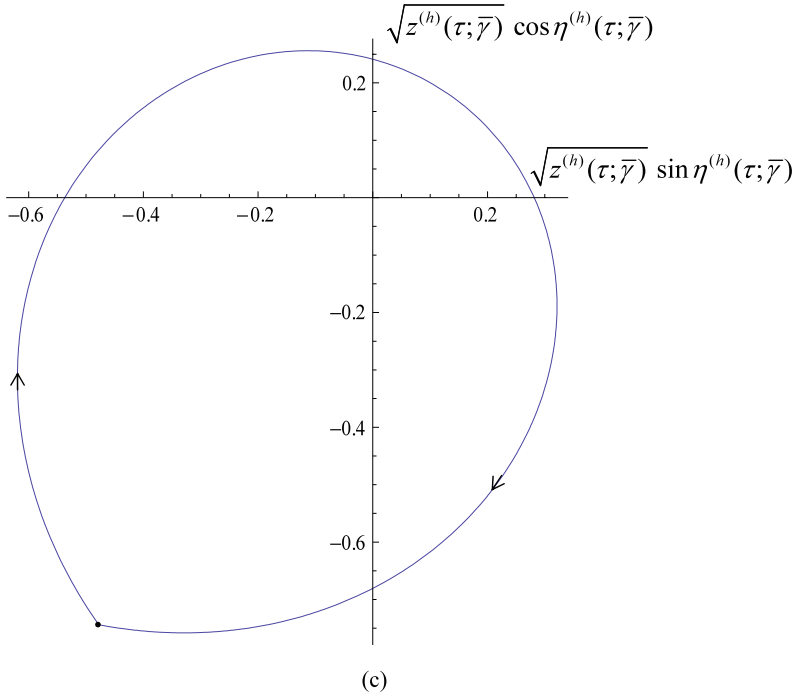

(c)

The homoclinic solution (36, 37) satisfies the initial conditions $z^{(h)}(0;\bar{\gamma}) = W_{cr}^2(\bar{\gamma})$ and $\eta^{(h)}(0;\bar{\gamma}) = 0$, and a representative example is depicted in Fig. 5. The additional homoclinic orbit corresponding to the case $z_0(\bar{\gamma}) < z_1(\bar{\gamma}) \leq W_{cr}^2(\bar{\gamma}) \leq z_2(\bar{\gamma})$ can be similarly computed in closed form but is not presented here.

By varying $\bar{\gamma}$ in the range $[0, \pi)$ (since $Q(z, W, \hat{F}, \bar{\gamma})$ is periodic in $\bar{\gamma}$ with period equal to 2π and is antisymmetric with respect to $\bar{\gamma} = \pi$), the unperturbed system (31) possesses two degenerate *homoclinic manifolds* (*tori*) Γ in $(\mathbb{C} \times S^1)$ space, and an unstable hyperbolic periodic orbit M. In Fig. 6, we depict one of the two degenerate homoclinic tori corresponding to the analytical solution (36, 37), as well as the hyperbolic periodic orbit M; only the torus in the range $0 \leq \bar{\gamma} \leq \pi$ is depicted, with the remaining part for $\pi \leq \bar{\gamma} \leq 2\pi$ being symmetric with respect to the plane $\bar{\gamma} = \pi$. Clearly, this highly degenerate structure is not expected to persist in the perturbed system (for $0 < \varepsilon \ll 1$) and, as shown below, its breakdown can lead to highly complex chaotic dynamics. In the following analysis, we study analytically the breakdown of the homoclinic manifolds in the perturbed system in order to prove the existence of chaotic orbits in the perturbed dynamics.

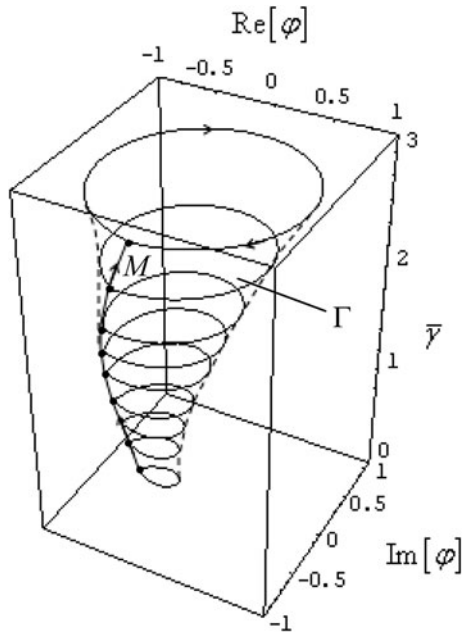

Fig. 6 Degenerate homoclinic torus of the unperturbed system (31) ($\varepsilon = 0$) for $\hat{F} = 0.1836$, $\hat{C} = 4/3$, and the unstable hyperbolic periodic orbit Γ (only the torus in the range $0 \leq \bar{\gamma} \leq \pi$ is depicted)

We now express the perturbed system (31) for $0 < \varepsilon \ll 1$ in perturbed Hamiltonian form. To this end, we express the complex amplitude as $\varphi(\tau) = x_1(\tau) + jx_2(\tau)$ and rewrite (31) in the following matrix form:

$$\left.\begin{aligned} \underline{x}' &= J\nabla H(\underline{x},\gamma;\underline{\mu}) + \varepsilon^{1/4}\underline{g}_x(\underline{x};\underline{\mu}) \\ \gamma' &= \varepsilon^{1/4} g_\gamma(\underline{x},\gamma) \end{aligned}\right\} (\underline{x},\gamma)\in R^2\times S^1 \tag{38}$$

In (38) $\underline{x}=(x_1,x_2)^T$, the ∇ operator is taken with respect to $\underline{x}$, $\underline{g}_x(\underline{x};\underline{\mu})=(-x_1\hat{\lambda}/2,-x_2\hat{\lambda}/2)^T$, $g_\gamma(\underline{x},\gamma)=\bar{B}$, and $\underline{\mu}=(\hat{\lambda},\hat{F})^T$ is a vector of parameters. The Hamiltonian function in (38) is given by

$$H(\underline{x},\gamma;\underline{\mu}) = \frac{x_1^2+x_2^2}{4} - \frac{3\hat{C}(x_1^2+x_2^2)^2}{32} + \frac{\hat{F}}{2}\left[x_1(1+\cos\gamma)+x_2\sin\gamma\right]$$

with

$$J=\begin{bmatrix} 0 & 1 \\ -1 & 0 \end{bmatrix}$$

For $\varepsilon=0$ and for every $\gamma\in S^1$, the unperturbed Hamiltonian system (38) is completely integrable with Hamiltonian $H(\underline{x},\gamma;\underline{\mu})$, it possesses an unstable hyperbolic equilibrium point which varies smoothly with γ, and it has a one-dimensional homoclinic manifold connecting the equilibrium point to itself; we represent the orbits along the homoclinic manifold as $\underline{x}=\underline{x}^{(h)}(\tau;\gamma)=(x_1^{(h)}(\tau;\gamma),x_2^{(h)}(\tau;\gamma))$, where

$$x_1^{(h)}(\tau;\gamma)=\sqrt{z^{(h)}(\tau;\gamma)}\cos\eta^{(h)}(\tau;\gamma)$$

$$x_2^{(h)}(\tau;\gamma)=\sqrt{z^{(h)}(\tau;\gamma)}\sin\eta^{(h)}(\tau;\gamma)$$

and $z^{(h)}(\tau;\gamma)$, $\eta^{(h)}(\tau;\gamma)$ are defined by (36, 37). By varying $\gamma\in[0,2\pi)$, the unperturbed system possesses a one-dimensional normally hyperbolic invariant manifold,

$$T=\left\{(\underline{x},\gamma)\in R^2\times S^1, \underline{x}=\underline{\sigma}(\gamma), \gamma\in S^1\right\}$$

where $\nabla H(\underline{\sigma}(\gamma),\gamma)=0$ and $\det[\nabla^2 H(\underline{\sigma}(\gamma),\gamma)]\neq 0$ which guarantees hyperbolicity of $\underline{\sigma}(\gamma)$ (cf. Fig. 6). Moreover, T has smooth two-dimensional stable and unstable invariant manifolds denoted by $W^s(T)$ and $W^u(T)$, respectively, which intersect (in fact, they completely coincide) in two two-dimensional homoclinic manifolds denoted by Γ (e.g., Fig. 6), and defined as

$$\Gamma=\left\{\left(\underline{x}=\underline{x}^{(h)}(-\tau_0;\gamma),\gamma\right)\in R^2\times S^1, \right.$$
$$\left.(\tau_0,\gamma)\in R\times S^1\right\}$$

where τ_0 parameterizes the one-dimensional homoclinic manifold for fixed γ.

The breakdown of the homoclinic manifolds Γ for $0<\varepsilon\ll 1$ was studied in [33]. In the perturbed system, there exists a $\gamma_0>0$ such that for $0<\gamma\leq\gamma_0$ the perturbed system possesses a one dimensional normally hyperbolic invariant manifold,

$$T_{\varepsilon^{1/4}}=\left\{(\underline{x},\gamma)\in R^2\times S^1, \underline{x}=\tilde{\underline{\sigma}}\left(\gamma;\varepsilon^{1/4}\right)\right.$$
$$\left.=\underline{\sigma}(\gamma)+O\left(\varepsilon^{1/4}\right), \gamma\in S^1\right\}$$

which is an $O(\varepsilon^{1/4})$ perturbation of T. Moreover, $T_{\varepsilon^{1/4}}$ has two-dimensional stable and unstable manifolds $W^s(T_{\varepsilon^{1/4}})$ and $W^u(T_{\varepsilon^{1/4}})$ which, if they intersect transversely, give rise to Smale horseshoes close to these intersections, and hence to chaotic orbits. Wiggins [33] proved that the distance between the perturbed manifolds in the normal direction at a point $(\tau_0,\gamma)\in\Gamma$ (of the unperturbed homoclinic manifolds) is given by

$$d\left(\tau_0,\gamma,\underline{\mu};\varepsilon^{1/4}\right) = \frac{\varepsilon^{1/4}M(\gamma;\underline{\mu})}{\|\nabla H(\underline{x}^{(h)}(-\tau_0),\gamma;\underline{\mu})\|} + O\left(\varepsilon^{1/2}\right) \tag{39a}$$

where the homoclinic Melnikov function $M(\gamma;\hat{\lambda})$ is defined by

$$M(\gamma;\underline{\mu}) = \int_{-\infty}^{\infty}\left[\langle\nabla H,\underline{g}_x\rangle + \left\langle\nabla H,\frac{\partial J\nabla H\int^\tau g_\gamma}{\partial\gamma}\right\rangle\right]_{(\underline{x}^{(h)}(\tau,\gamma),\underline{\mu})} d\tau \tag{39b}$$

and $\langle\cdot,\cdot\rangle$ denotes the Euclidean inner product. Hence, the homoclinic Melnikov function is computed only based on the unperturbed homoclinic solution.

The existence of chaotic orbits in the perturbed system is then proved by the following theorem.

Theorem 1 [33] *Suppose that there exists a point* $(\gamma,\hat{\lambda})=(\gamma^*,\hat{\lambda}^*)$ *such that*

(i) $M(\gamma^*;\hat{\lambda}^*)=0$
(ii) $\nabla M(\gamma^*;\hat{\lambda}^*)$ *is of rank* 1

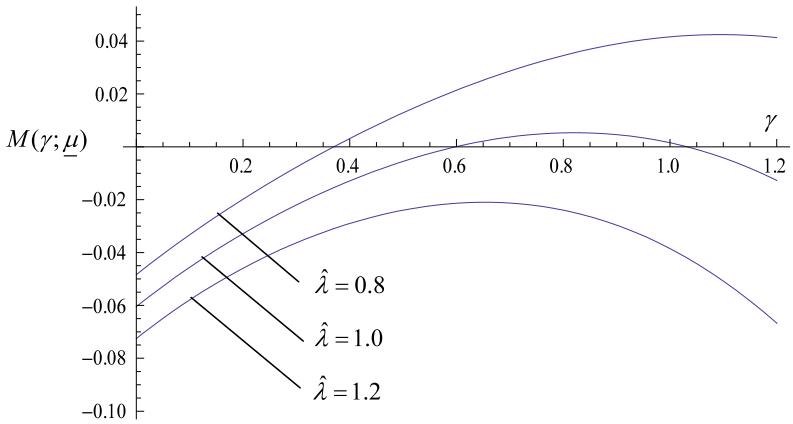

Fig. 7 Plot of the homoclinic Melnikov function $M(\gamma;\hat{\lambda},\bar{B}=-1/1.79958)$ versus γ for $\hat{\lambda}=0.8$, 1.0, 1.2

Then for sufficiently small $\varepsilon^{1/4}$, *the perturbed invariant manifolds* $W^s(T_{\varepsilon^{1/4}})$ *and* $W^u(T_{\varepsilon^{1/4}})$ *intersect transversely near* $(\gamma^*,\hat{\lambda}^*)$.

Then we can invoke Birkhoff's homoclinic theorem [33] to prove that transverse intersections of the stable and unstable manifolds of $T_{\varepsilon^{1/4}}$ generate chaotic Smale horseshoe maps in neighborhoods of the transverse homoclinic intersections, and hence to countable infinities of unstable orbits of every possible period, uncountable infinities of unstable orbits and dense orbits. We note that the fact that in our case the perturbation of the homoclinic manifold is slowly varying does not restrict the homoclinic Melnikov analysis. In fact, in the terminology of Wiggins [33], system (38) is a Type-II dynamical system with $I=0$, $\Omega(x,I)=0$ and $\dot{\theta}\ll 1$. A similar application of Melnikov analysis for the case of a parametrically forced pendulum with a slowly varying frequency is provided in [33].

Substituting the expression for the unperturbed homoclinic solution (36, 37) in (39b) the homoclinic Melnikov function is expressed as

$$
\begin{aligned}
&M(\gamma;\underline{\mu})\\
&=\int_{-\infty}^{\infty}\Big\{-\big(\hat{\lambda}/4\big)\big(x_1^2+x_2^2\big)+\big(3\hat{C}\hat{\lambda}/16\big)\big(x_1^2+x_2^2\big)^2\\
&\quad-\big(\hat{\lambda}\hat{F}/4\big)\big[x_1(1+\cos\gamma)+x_2\sin\gamma\big]\\
&\quad+\big(\bar{B}\hat{F}\tau/2\big)\big\{\big[(x_1/2)-\big(3\hat{C}x_1/8\big)\big(x_1^2+x_2^2\big)\\
&\quad+\hat{F}(1+\cos\gamma)\big]\cos\gamma\\
&\quad+\big[(x_2/2)-\big(3\hat{C}x_2/8\big)\big(x_1^2+x_2^2\big)\\
&\quad+\big(\hat{F}/2\big)\sin\gamma\big]\sin\gamma\big\}\Big\}_{(\underline{x}^{(h)}(\tau,\gamma),\underline{\mu})}d\tau \qquad (40)
\end{aligned}
$$

Direct numerical computations prove that $M(\gamma;\underline{\mu})$ indeed possess simple roots in terms ofγ, so the existence of transverse homoclinic intersections in the dynamics of the perturbed system (31) can be rigorously proved by application of Birkhoff's homoclinic theorem. As an example, for $\hat{F}=0.1786$, $\hat{C}=4/3$, and $\gamma=0.6$ the homoclinic Melnikov function is computed as $M=-0.107073\hat{\lambda}-0.163227\bar{B}$. Hence, for $\hat{\lambda}/\bar{B}=-1.79958$, the Melnikov function has a zero; the proof that this is a simple zero can be verified by setting $\hat{\lambda}=1$ and plotting $M(\gamma;\hat{\lambda}=1,\bar{B}=-1/1.79958)$ versus γ as depicted in Fig. 7. Moreover, by varying $\hat{\lambda}$ for fixed values of $\hat{F}=0.1786$, $\hat{C}=4/3$, and $\bar{B}=-1/1.79958$, we may *predict* the generation of chaotic orbits in the dynamics as we move from the case where no transverse homoclinic intersections occur ($\hat{\lambda}=1.2$), to the case where transverse homoclinic intersections take place ($\hat{\lambda}=1.0$ and $\hat{\lambda}=0.8$), as shown in Fig. 7. This analytical result based on homoclinic Melnikov theory is verified by direct numerical integrations of the reduced model (31), as depicted in Fig. 8. In this figure, we present direct numerical simulations of system (31) for $\hat{F}=0.1786$, $\hat{C}=4/3$, $\bar{B}=-1/1.79958$, $\varepsilon^{1/4}=0.05$, and $\hat{\lambda}=1.2$, 1.0, and 0.8. For stronger damping (cf. Fig. 8c), the dynamics settles into a low-amplitude regular motion, whereas for lighter damping (cf. Figs. 8a and 8b), the system executes chaotic oscillations; these numerical results are fully compatible with and verify the results of the analytical homoclinic Melnikov study.

The analysis of this section proves the occurrence of chaotic dynamic interactions between traveling waves in the chain and the weakly damped strongly

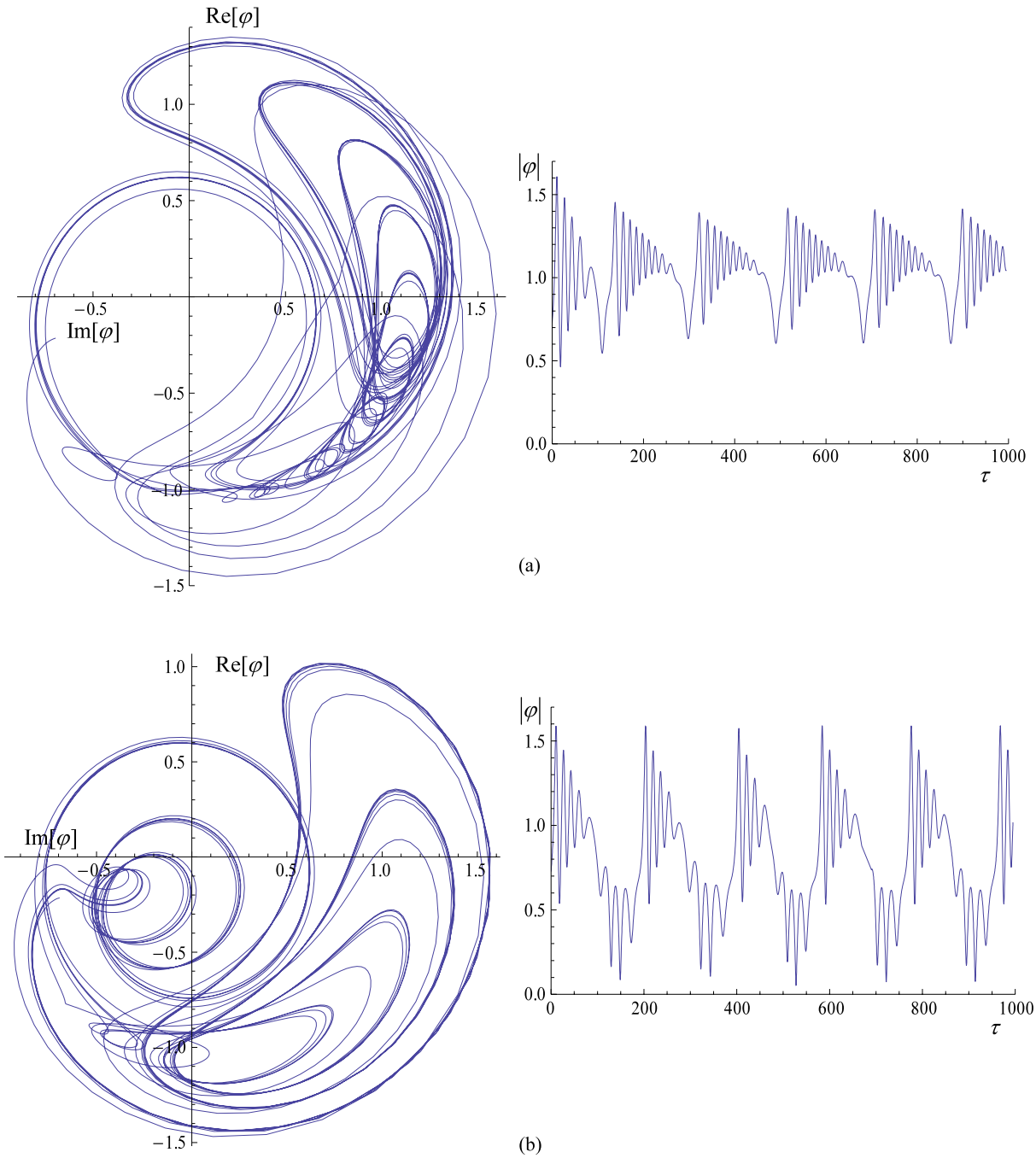

Fig. 8 Direct numerical simulations of the reduced model (31) for $\hat{F} = 0.1836, \hat{C} = 4/3, \bar{B} = -1/1.79958, \varepsilon^{1/4} = 0.05$, and (**a**) $\hat{\lambda} = 0.8$, (**b**) $\hat{\lambda} = 1.0$, (**c**) $\hat{\lambda} = 1.2$

nonlinear attachment. As mentioned by a reviewer, there is no guarantee that the chaotic dynamics forms an attractive set, so we cannot prove persistence of the chaotic dynamics with increasing time. Hence, it is possible that only transient chaos exists in this case; our results, however, do indicate the occurrence of complex dynamic behavior, and prove nonintegrability of the dynamics in the system.

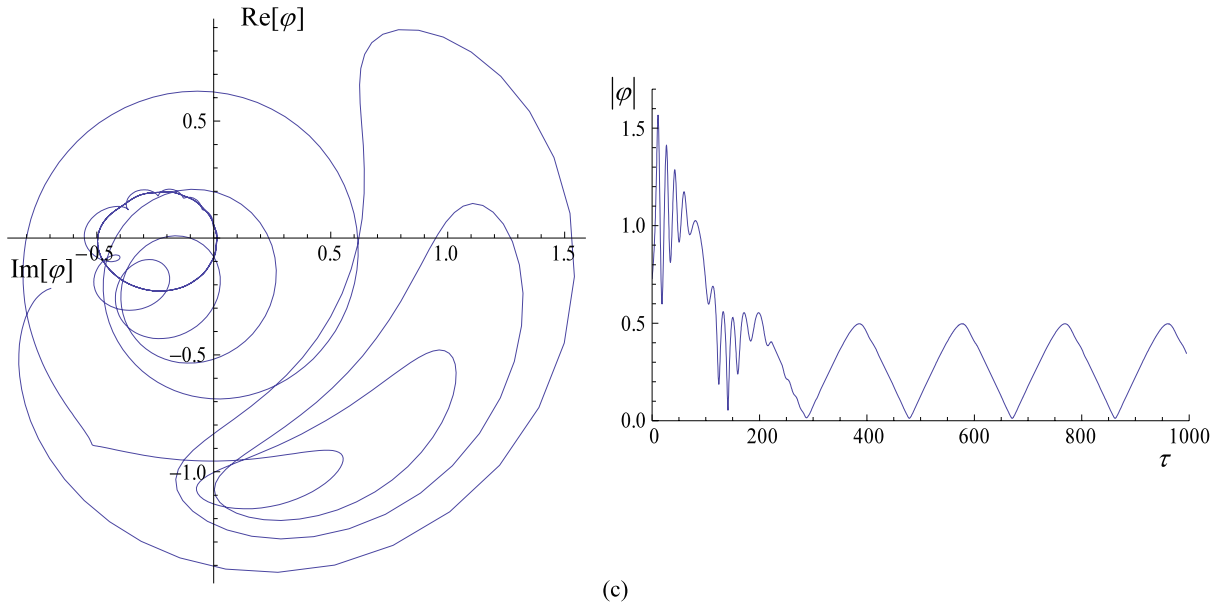

(c)

Fig. 8 (*Continued*)

In the next section, we provide a note that proves that in the limit of no damping the traveling wave-attachment interaction can give rise to a countable infinity of subharmonic orbits. This is performed by constructing appropriate subharmonic Melnikov functions as outlined in [33].

5 A note on subharmonic motions

Depending on the initial conditions of the nonlinear attachment and the frequency and amplitude of the traveling wave of the lattice, a countable infinity of subharmonic resonances may occur, whereby the frequency of the attachment is tuned to a rational relation with respect to the frequency of the traveling wave. To show this, we reconsider the reduced model (16) and express it in terms of action-angle variables [24]. Setting damping equal to zero, $\hat{\lambda} = 0$, and omitting terms of $O(\varepsilon)$, the reduced model can be expressed in the following autonomous form:

$$\begin{aligned} I' &= -\varepsilon^{1/2}\hat{f}\frac{3I^{1/3}\pi(\sin\theta_1+\sin\theta_2)}{2K(1/2)\Lambda\Xi}\frac{\mathrm{sn}\,\mathrm{dn}}{\mathrm{cn}^4+2\mathrm{sn}^2\mathrm{dn}^2} \\ &\equiv \varepsilon^{1/2}\tilde{f}_1(I,\phi,\theta_1,\theta_2) \\ \phi' &= \tilde{\omega}(I)-\varepsilon^{1/2}\hat{f}\frac{\pi^2 I^{-2/3}(\sin\theta_1+\sin\theta_2)}{4K^2(1/2)\Lambda\Xi} \\ &\quad\times\frac{\mathrm{cn}}{\mathrm{cn}^4+2\mathrm{sn}^2\mathrm{dn}^2} \\ &\equiv \tilde{\omega}(I)+\varepsilon^{1/2}\tilde{f}_2(I,\phi,\theta_1,\theta_2) \\ \theta_1' &= 1 \\ \theta_2' &= \varepsilon^{1/4}\bar{B} \end{aligned} \tag{41a}$$

with initial conditions,

$$\begin{aligned} I^{2/3}(0) &= \frac{-W\pi}{2^{1/2}\Lambda\Xi K(1/2)} > 0, \\ \phi(0) &= \phi_0, \theta_1(0) = \theta_{10}, \theta_2(0) = \theta_{20} \end{aligned} \tag{41b}$$

In (41a), sn, cn and dn are Jacobi elliptic functions with arguments $[2K(1/2)(\phi+\pi/2)/\pi, 1/2]$, $K(1/2)$ is the complete elliptic integral of the first kind [2], and the various parameters are defined as $\tilde{\omega}(I) = \Xi I^{1/3}$, $\Lambda = (4C)^{-1/6}[3\pi/K(1/2)]^{1/3}$ and $\Xi = [3\pi^4 C/8K^4(1/2)]^{1/3}$; moreover, we have rescaled the amplitude of the traveling wave as $\hat{F} = \varepsilon^{1/2}\hat{f}$, so that the initial condition becomes $W \equiv \varepsilon^{1/2}\hat{f} - V < 0$.

Hence, the reduced model (16) has been transformed to a dynamical system on a 3-torus $(I, \phi, \theta_1, \theta_2) \in R^+ \times S^1 \times S^1 \times S^1$, possessing two fast frequencies equal to $\tilde{\omega}(I) + O(\varepsilon^{1/2})$ and 1, and a slow frequency equal to $\varepsilon^{1/4}\bar{B}$. The subharmonic orbits of system (41) can be studied in the limit $0 < \varepsilon \ll 1$ by

invoking the following *internal resonance condition* between the two fast frequencies of the problem:

$$m\tilde{\omega}(I) - n = 0 \quad \Rightarrow$$
$$I = \left(\frac{n}{m\,\Xi}\right)^3 \equiv I^{(m/n)}, \quad n, m \in N^+$$

This couples the two fast frequencies of the reduced problem and defines an $(m:n)$ *resonance manifold* for the dynamics. Moreover, we restrict the dynamics in an $O(\varepsilon^{1/4})$ neighborhood of the $(m:n)$ resonance manifold by constructing a *local* model close to this manifold. This is performed by introducing the new angle $\rho = m\phi - n\theta$ and the local action variable $\xi(\theta)$ defined by $I(\theta) = I^{(m/n)} + \varepsilon^{1/4}\xi(\theta)$. This local study, however, which can be used to reveal the rich structure of subharmonic bifurcations that occur close to the $(m:n)$ resonance manifold will be investigated in detail in another work. In this note, we will adopt an alternative *global* approach (in the sense that our analysis will not be restricted in a neighborhood of a resonance manifold) in order to show how one can prove the existence of a countable infinity of subharmonic orbits in system (41) through the use of subharmonic Melnikov analysis.

Following [33], we rewrite system (41a) in the slightly more general form,

$$\begin{aligned} I' &= \varepsilon^{1/2}\tilde{f}_1(I, \phi, \theta_1, \theta_2) \\ \phi' &= \tilde{\omega}(I) + \varepsilon^{1/2}\tilde{f}_2(I, \phi, \theta_1, \theta_2) \\ \theta_1' &= 1 \\ \theta_2' &= \beta \end{aligned} \tag{42}$$

which allows for the existence of three fast frequencies in the dynamics of the strongly coupled chain. Clearly, the unperturbed dynamics (corresponding to $\varepsilon = 0$) takes place on a 3-torus which is foliated by a continuous families of periodic and quasiperiodic orbits. We wish to study how the $O(\varepsilon^{1/2})$ perturbative terms in (42) affect the dynamics on the torus.

Following [33], a $(m:n:p)$ *resonant 3-torus* of the unperturbed system (42) corresponds to the value of the action for which the following relation between the three frequencies of the system is satisfied,

$$\begin{aligned} &\tilde{\omega}\big(I^{(m/n/p)}\big) = n/p = n\beta/m \quad \Rightarrow \\ &n\tilde{T}\big(I^{(m/n/p)}\big) = p2\pi = mT \end{aligned} \tag{43}$$

where $\tilde{T}(I^{(m/n/p)}) = 2\pi/\tilde{\omega}(I^{(m/n/p)}) \equiv \tilde{T}^{m/n/p}$ and $T = 2\pi/\beta$. Since the nondegeneracy condition $\tilde{\omega}'(I) \neq 0$ is satisfied for the system considered here, there is a unique solution $I = I^{(m/n/p)}$ of (44) for every triplet $(m, n, p) \in \mathbb{N}^{+3}$. Hence, there is a countable infinity of resonant 3-tori (corresponding to subharmonic orbits in the unperturbed system) and an uncountable infinity of non-resonant 3-tori (corresponding to quasi-periodic orbits in the unperturbed system).

Using subharmonic Melnikov theory, we will study preservation of subharmonic orbits in the perturbed system. To do this, we consider the global cross section in the phase space of the dynamics,

$$\begin{aligned} \Sigma^{\theta_{20}} = \big\{&(I, \phi, \theta_1, \theta_2) \in R^+ \times S^1 \times S^1 \times S^1, \\ &\theta_2 = \theta_{20} \in [0, 2\pi)\big\} \end{aligned}$$

and the Poincare' map,

$$\begin{aligned} &P_\varepsilon : \Sigma^{\theta_{20}} \to \Sigma^{\theta_{20}}, \\ &\big(I(0), \phi(0), \theta_1(0)\big) \to \big(I(T), \phi(T), \theta_1(T)\big) \end{aligned}$$

so that the m-th iterate of the Poincare' map is defined as

$$\begin{aligned} &P_\varepsilon^m : \Sigma^{\theta_{20}} \to \Sigma^{\theta_{20}}, \\ &\big(I(0), \phi(0), \theta_1(0)\big) \to \big(I(mT), \phi(mT), \theta_1(mT)\big) \end{aligned}$$

Returning to the dynamical system (42) we approximate the perturbed solutions in the following series form:

$$\begin{aligned} I(\tau) &= I_0 + \varepsilon^{1/2} I_1(\tau) + O(\varepsilon) \\ \phi(\tau) &= \tilde{\omega}(I_0)\tau + \phi_0 + \varepsilon^{1/2}\phi_1(\tau) + O(\varepsilon) \\ \theta_1(\tau) &= \tau + \theta_{10} \\ \theta_2(\tau) &= \beta\tau + \theta_{20} \end{aligned} \tag{44}$$

where general initial conditions were assumed. The leading order approximations can be computed by substituting (44) in (42) and matching $O(\varepsilon^{1/2})$ terms. Then we can approximate the corrections to the action and angle variables after time mT as follows [33]:

$$\begin{aligned} &I_1(mT) \\ &\quad = \int_0^{mT} \tilde{f}_1\big(I_0, \tilde{\omega}(I_0)\xi + \phi_0, \xi + \theta_{10}, \beta\xi + \theta_{20}\big)d\xi \\ &\quad \equiv M_1\,(I_0, \phi_0; \theta_{10}, \theta_{20}) \\ &\phi_1(mT) \end{aligned}$$

$$
\begin{aligned}
&= \tilde{\omega}'(I_0) \int_0^{mT} \int_0^{\xi} \tilde{f}_1\big(I_0, \tilde{\omega}(I_0)\zeta + \phi_0, \zeta + \theta_{10}, \\
&\qquad\qquad \beta\zeta + \theta_{20}\big) d\zeta\, d\xi \\
&\quad + \int_0^{mT} \tilde{f}_2\big(I_0, \tilde{\omega}(I_0)\xi + \phi_0, \xi + \theta_{10}, \\
&\qquad\qquad \beta\xi + \theta_{20}\big) d\xi \\
&\equiv M_2\,(I_0, \phi_0; \theta_{10}, \theta_{20})
\end{aligned}
\tag{45}
$$

This enables us to analytically approximate the m-th iterate of the Poincare' map as follows:

$$
\begin{aligned}
&P_\varepsilon^m : \Sigma^{\theta_{20}} \to \Sigma^{\theta_{20}}, \\
&\big(I(0), \phi(0)\big) \\
&\quad \to \big(I_0 + \varepsilon^{1/2} M_1(I_0, \phi_0; \theta_{10}, \theta_{20}), \\
&\qquad \tilde{\omega}(I_0) mT + \phi_0 + \varepsilon^{1/2} M_2\big(I_0, \phi_0; \theta_{10}, \theta_{20}\big)\big) \\
&\qquad + O(\varepsilon)
\end{aligned}
\tag{46}
$$

where the trivial dependence on the angle θ_1 was eliminated.

We note that if we set $I_0 = I^{(m/n/p)}$ the functions $\tilde{f}_1$ and $\tilde{f}_2$ become periodic in τ with period equal to mT; it follows that the $O(\varepsilon^{1/2})$ perturbations $I_1(\tau)$ and $\phi_1(\tau)$ for the $(m:n:p)$ resonant 3-torus are also mT-periodic in τ. For the $(m:n:p)$ resonant 3-torus, we define the following subharmonic Melnikov functions:

$$
\begin{aligned}
&M_{1,2}\big(I^{(m/n/p)}, \phi_0; \theta_{10}, \theta_{20}\big) \\
&\quad \equiv M_{1,2}^{(m/n/p)}\big(I^{(m/n/p)}, \phi_0; \theta_{10}, \theta_{20}\big)
\end{aligned}
\tag{47}
$$

The preservation of subharmonic orbits in the perturbed system is then established by the following theorem.

Theorem [33] *Suppose that there exists a* $\phi_0 = \phi^{(m/n/p)}$, *such that*

$$
\begin{aligned}
&M_1\big(I^{(m/n/p)}, \phi^{(m/n/p)}; \theta_{10}, \theta_{20}\big) = 0 \quad \text{and} \\
&\left\{\tilde{\omega}' \frac{\partial M_1^{(m/n/p)}}{\partial \phi_0}\right\}_{(I^{(m/n/p)}, \phi^{(m/n/p)})} = 0
\end{aligned}
\tag{48}
$$

Then for $0 < \varepsilon < \bar{\varepsilon}(n, p)$, *the Poincare' map* P_ε *has a pair of equilibrium points of period* m, *one of which is stable and the other unstable. This implies that a stable-unstable pair of subharmonic orbits of period* mT *is preserved in the perturbed system* (42).

By applying this theorem, one can prove the preservation in the perturbed system (42) of a countable infinity of stable subharmonic orbits of arbitrarily large periods. We note that the zeros $(I^{(m/n/p)}, \phi^{(m/n/p)})$ of the subharmonic Melnikov function determines the corresponding initial conditions W and ϕ_0 for the reduced model (41a) through relations (41b), after taking $\theta_{10} = \theta_{20} = 0$.

In addition, if the model (42) is expressed in Cartesian form,

$$
\underline{x}' = J \nabla H(\underline{x}) + \varepsilon^{1/2} \underline{g}(\underline{x}, \tau, \beta\tau)
\tag{49}
$$

where $\underline{x} = (x_1, x_2)^T$, $\underline{g} = (g_1, g_2)^T$, and the notation of the previous section is employed, the Melnikov function M_1 can be expressed in the following form which is amenable to direct analytical evaluation:

$$
\begin{aligned}
&M_1^{(m/n/p)} \\
&\quad = M_1^{(m/n/p)}\,(\alpha, \tau_0; \theta_{10}, \theta_{20}) \\
&\quad = \tilde{\omega}^{-1}\big(I^{(m/n/p)}\big) \int_0^{mT} \left\{\frac{\partial H}{\partial x_1} g_1\right. \\
&\qquad \left. + \frac{\partial H}{\partial x_2} g_2\right\}_{(\underline{x}^\alpha(\tau;\tau_0), \tau+\tau_0+\theta_{10}, \beta\tau+\beta\tau_0+\theta_{20})} d\tau
\end{aligned}
\tag{50}
$$

In (50), $\underline{x}^\alpha(\tau; \tau_0)$ is the unperturbed solution of period $\tilde{T}(I^{(m/n/p)}) = 2\pi/\tilde{\omega}(I^{(m/n/p)}) \equiv \tilde{T}^{m/n/p}$ (which can be computed explicitly by quadratures in terms of Jacobi elliptic functions), index α parameterizes the corresponding action (energy) of the unperturbed periodic orbit, τ_0 is the initial condition on the periodic orbit, and the initial angles are assigned zero values, i.e., $\theta_{10} = \theta_{20} = 0$. Using the alternative expression (50), we can explicitly compute the Melnikov function in terms of the unperturbed periodic orbit and prove that it possesses simple zeros in a way similar to our homoclinic Melnikov analysis of the previous section. Then the preservation of the family of subharmonic orbits in the perturbed system can be rigorously studied.

6 Concluding remarks

We studied strongly nonlinear dynamical interactions between traveling waves propagating in a linear lattice and a lightweight essentially nonlinear local attachment (defect). Through the use of the Green's function

of the lattice at the point of attachment to the nonlinear oscillator, and by considering only leading-order terms in the dynamic interaction we reduced the dynamics to a strongly nonlinear damped oscillator with two-frequency harmonic forcing; one of the frequencies of the excitation was characteristic of the traveling wave, whereas the other accounted for local lattice effects, i.e., for the linear grounding stiffness of each particle of the lattice. A third frequency characterized the nonlinear oscillation of the attachment, and in contrast to the previous two was energy-dependent.

We analyzed the dynamics of the reduced model in the limit of small attachment mass and for weak interparticle coupling in the lattice. We showed that below a damping threshold the nonlinear attachment executes relaxation oscillations. These motions were analytically studied by constructing slow invariant manifolds (SIMs) of the dynamics. In the limit of weak or no damping, we proved the existence of subharmonic and chaotic oscillations through the use of subharmonic and homoclinic Melnikov theory.

The ideas and methodologies adopted in this work can be applied to study nonlinear dynamic interactions of traveling or standing (near-field) waves in linear periodic media with local nonlinear attachments or defects. Another possible extension is in the area of soliton-defect interaction in nonlinear periodic media; however, an alternative reduction process should be developed in that case in order to derive a reduced order model that fully captures the leading order dynamic interaction between the solitary waves and the attachment.

References

1. Akozbek, N., John, S.: Optical solitary waves in two- and three-dimensional nonlinear photonic band-gap structures. Phys. Rev. E **57**(2), 2287–2320 (1998)
2. Byrd, P.F., Friedman, M.D.: Handbook of Elliptic Integrals for Engineers and Physicists. Springer, Berlin (1954)
3. Chen, W., Mills, D.: Gap solitons and the nonlinear optical response of superlattices. Phys. Rev. Lett. **58**(2), 160–164 (1987)
4. Dannefaer, S.: Lattice relaxation at V^-, NV^- and NVN^- defects in diamond investigated by positron annihilation. J. Phys. Condens. Matter **21**, 175412 (2009)
5. Daraio, C., Nesterenko, V.F., Herbold, E.B., Jin, S.: Energy trapping and shock disintegration in a composite granular medium. Phys. Rev. Lett. **96**, 058002 (2006)
6. Fedele, F., Jianke, Y., Chen, Z.: Defect modes in one-dimensional photonic lattices. Opt. Lett. **30**, 1506–1508 (2005)
7. Fei, Z., Kivshar, Y.S., Vazquez, L.: Resonant kink-impurity interactions in the ϕ^4 model. Phys. Rev. A **46**, 5214–5220 (1992)
8. Forinash, K., Peyrard, M., Malomed, B.: Interaction of discrete breathers with impurity modes. Phys. Rev. E **49**, 3400–3411 (1994)
9. Gendelman, O.V., Gourdon, E., Lamarque, C.-H.: Quasiperiodic energy pumping in coupled oscillators under periodic forcing. J. Sound Vib. **294**, 651–662 (2006)
10. Gendelman, O.V., Starosvetsky, Y.: Quasi-periodic response regimes of linear oscillator coupled to nonlinear energy sink under periodic forcing. J. Appl. Mech. **74**, 325–331 (2007)
11. Gendelman, O.V., Starosvetsky, Y., Feldman, M.: Attractors of harmonically forced linear oscillator with attached nonlinear energy sink I: Description of response regimes. Nonlinear Dyn. **51**, 31–46 (2008)
12. Goodman, R.H., Holmes, P.J., Weinstein, M.I.: Interaction of sine-Gordon kinks with defects: phase space transport in a two-mode model. Physica D **161**, 21–44 (2002)
13. Goodman, R.H., Holmes, P.J., Weinstein, M.I.: Strong NLS soliton–defect interactions. Physica D **192**, 215–248 (2004)
14. Gradshteyn, I.S., Ryzhik, I.M.: Table of Integrals, Series and Products. Academic Press, New York (1980)
15. Karazhanov, S., Zhang, Y., Wang, L.-W., Mascarenhas, A., Deb, S.: Resonant defect states and strong lattice relaxation of oxygen vacancies in WO3. Phys. Rev. B **68**(23), 233204 (2003)
16. Kivshar, Y.S., Gredeskul, S.A., Sánchez, A., Vázquez, L.: Localization decay induced by strong nonlinearity in disordered systems. Phys. Rev. Lett. **64**(15), 1693–1696 (1990)
17. Lang, D.V., Logan, R.A.: Large-Lattice-Relaxation model for persistent photoconductivity in compound semiconductors. Phys. Rev. Lett. **39**, 635–639 (1977)
18. Lazarov, B.S., Jensen, J.S.: Low-frequency band gaps in chains with attached nonlinear oscillators. Int. J. Non-linear Mech. **42**, 1186–1193 (2007)
19. Manevitch, L.I.: Complex representation of dynamics of coupled nonlinear oscillators. In: Uvarova, L., Arinstein, A., Latyshev, A. (eds.) Mathematical Models of Non-Linear Excitations, Transfer Dynamics and Control in Condensed Systems and Other Media. Kluwer Academic/Plenum, Norwell/New York (1999)
20. Mead, D.J.: Wave propagation and natural modes in periodic systems: I. Mono-coupled systems. J. Sound Vib. **40**(1), 1–18 (1975)
21. Muratov, L., Little, S., Yang, Y., Cooper, B., Myers, T., Wills, J.: Predicted lattice relaxation around point defects in zinc selenide. Phys. Rev. B **64**, 035206 (2001)
22. Nayfeh, A.H., Mook, D.T.: Nonlinear Oscillations. Wiley-Interscience, New York (1979)
23. Nesterenko, V.F., Daraio, C., Herbold, E.B., Jin, S.: Anomalous wave reflection at the interface of two strongly nonlinear granular media. Phys. Rev. Lett. **95**, 158702 (2005)
24. Percival, I., Richards, D.: Introduction to Dynamics. Cambridge University Press, Cambridge (1982)
25. Rothos, V., Vakakis, A.F.: Dynamic interaction of traveling waves propagating in an infinite linear chain with a local essentially nonlinear attachment. Wave Motion **46**, 174–188 (2009)

26. Sapsis, T., Vakakis, A.F., Gendelman, O.V., Bergman, L.A., Kerschen, G., Quinn, D.D.: Efficiency of targeted energy transfers in coupled nonlinear oscillators associated with 1:1 resonance captures: Part II, analytical study. J. Sound Vib. **325**, 297–320 (2009)
27. Shinozuka, Y., Karatsu, T.: Transient lattice vibration induced by coherent carrier captures at a deep-level defect and the effect on defect reactions. Physica B **273–274**, 999–1002 (1999)
28. Vakakis, A.F., Gendelman, O.V.: Energy pumping in nonlinear mechanical oscillators: Part II—Resonance capture. J. Appl. Mech. **68**, 42–48 (2001)
29. Vakakis, A.F., Gendelman, O., Bergman, L.A., McFarland, D.M., Kerschen, G., Lee, Y.S.: Nonlinear Targeted Energy Transfer in Mechanical and Structural Systems. Springer, Berlin (2008)
30. Verhulst, F.: Methods and Applications of Singular Perturbations. Springer, Berlin (2005)
31. Wang, Y.Y., Lee, K.H.: Propagation of a disturbance in a chain of interacting harmonic oscillators. Am. J. Phys. **41**, 51–54 (1973)
32. Watson, G.N.: A Treatise on the Theory of Bessel Functions. Cambridge University Press, Cambridge (1980)
33. Wiggins, S.: Global Bifurcations and Chaos. Springer, Berlin (1988)